# Comparing the optimal signal conditions for recording cubic and quadratic distortion product otoacoustic emissions

Lin Bian[a] and Shixiong Chen
*Auditory Physiology Lab, 3430 Coor Hall, Department of Speech and Hearing Science, Arizona State University, Tempe, Arizona 85287-0102*

(Received 22 July 2008; revised 24 September 2008; accepted 24 September 2008)

Odd- and even-order distortion products (DPs), evoked by two primary tones ($f_1, f_2, f_1 < f_2$), represent different aspects of cochlear nonlinearity. The cubic and quadratic difference tones (CDT $2f_1 - f_2$ and QDT $f_2 - f_1$) are prominent representatives of the odd and even DPs. Distortion product otoacoustic emissions (DPOAEs) were measured within a primary level ($L_1, L_2$) space over a wide range of $f_2/f_1$ ratios to compare the optimal signal conditions for these DPs. For CDT, the primary level difference decreased as $L_1$ increased with a rate proportional to the $f_2/f_1$ ratio. Moreover, the optimal ratio increased with $L_1$. A set of two formulas is proposed to describe the optimal signal conditions. However, for a given level of a primary, increasing the other tone level could maximize the QDT amplitude. The frequency ratio at the maximal QDT was about 1.3 and quite constant across different primary levels. A notch was found in the QDT amplitude at the $f_2/f_1$ ratio of about 1.22–1.25. These opposite behaviors suggest that the optimal recording conditions are different for CDT and QDT due to the different aspects in the cochlear nonlinearity. Optimizing the DPOAE recordings could improve the reliability in clinical or research practices.
 [DOI: 10.1121/1.3001706]

PACS number(s): 43.64.Jb, 43.64.Kc, 43.64.Bt, 43.64.Yp [BLM] Pages: 3739–3750

## I. INTRODUCTION

Our inner ears are nonlinear acoustic transducers where distortions are normal by-products of the conversion of sound into bioelectrical signals. The source of distortion is thought to be within the transduction process of outer hair cells (OHCs), since these cells respond to changes in membrane voltage with mechanical motion in either the cell body (Liberman *et al.*, 2002) or the hair bundles (Kennedy *et al.*, 2005). The OHC transduction shows a saturating nonlinearity and the resulting motile responses provide a mechanical feedback that can enhance hearing sensitivity and frequency selectivity. When stimulated by two tones ($f_1, f_2, f_2 > f_1$), the inner ear can produce a family of distortion products (DPs) in various combinations of the primary frequencies, $mf_1 \pm nf_2$. Depending on the sum of integers $m$ and $n$, the DPs can be classified into two categories, odd- and even-order DPs. They reflect different aspects of the nonlinear transducer characteristics of OHCs in the overlapped region of traveling waves initiated by two pure tones. Odd-order DPs are relatively large at low primary levels, and representing the transducer gain of hair cells. In contrast, even-order DPs are only measurable at moderately high stimulus levels, and thus may reflect the saturation or compression of hair cell transducers. These DPs in mechanical vibrations of hair cells can propagate out of the inner ear and are measurable in the ear canal as faint sounds or distortion product otoacoustic emissions (DPOAEs). Therefore, DPOAEs provide a noninvasive tool to assess the functional status of the inner ear OHCs.

Given the possibility that DPOAEs can be used to evaluate the transducer characteristics of OHCs, the current clinical application is, however, limited to hearing screening (Lonsbury-Martin and Martin, 2003) where normal or abnormal hearing is judged by the presence or absence of emissions. Quantitative utilities, such as hearing threshold estimates, cochlear efferent function evaluation, and input/output growth functions, are restricted to mostly research settings. One reason for the limited use of DPOAEs is the large variability in measurements. Among other factors (Garner, 2008), such as hearing sensitivity, middle ear transmission, and inner ear reflections, a source of the variability can be attributed to less optimized signal conditions of the primary tones (Johnson *et al.*, 2006; Mills *et al.*, 2007) that cannot evoke the largest DPOAEs. Since DP levels are correlated with the nonlinear characteristics of cochlear transduction (Lukashkin and Russell, 1999; Fahey *et al.*, 2000; Bian *et al.*, 2002; Bian, 2004), maximizing DPOAE magnitudes can improve the signal-to-noise ratio (SNR) so that more accurate estimates of cochlear function are possible. Therefore, there is a need for standardizing (Mills *et al.*, 2007) or individualizing (Neely *et al.*, 2005) the measurement procedures. Optimizing the recording conditions for DPOAEs is still an ongoing research effort.

The signal conditions for recording DPOAEs include the $f_2/f_1$ frequency ratio and the levels of two primary tones ($L_1$ and $L_2$). The $f_2$ is usually predetermined for evaluating the cochlear function at a specific frequency of interest, because the overlapped region of the two-tone excitation patterns on cochlear partition is very close to the $f_2$ place. The frequency $f_1$ can be determined by selecting an appropriate $f_2/f_1$ ratio. In current clinical practice, a value of 1.22 is commonly adopted for $f_2/f_1$ ratio regardless of frequency and level.

[a]Electronic mail: lin.bian@asu.edu

However, the optimal ratio can range from 1.2 to 1.3 with increase in primary levels and $f_2$ (Moulin, 2000; Johnson *et al.*, 2006). Thus, for a certain $f_2$, selecting the frequency ratio is tied with the choice of primary levels. Currently, the decision on signal levels is an independent process and often a simple strategy of $L_1$ being 5–10 dB greater than $L_2$ is used. However, studies on DPOAE amplitude within a complete $L_1 \times L_2$ parameter space indicate that the primary level difference ($\Delta L = L_1 - L_2$) is also level dependent with greater deviations towards lower levels (e.g., Whitehead *et al.*, 1995). The optimal $L_1$ as a linear deviation from $L_2$ is refined with an empirical formula (Kummer *et al.*, 2000) given the observation that $\Delta L$ diminishes at 65 dB SPL. This primary level optimization allows a more accurate measurement of DPOAE amplitudes at low stimulus levels for estimating hearing sensitivity (Kummer *et al.*, 1998). Another relation between the optimal $L_1$ and $L_2$ is proposed by Johnson *et al.* (2006) which takes $f_2$ into account. However, none of the approaches considers the inter-relation between the primary levels and the $f_2/f_1$ ratio. The interaction between frequency ratio and primary levels on DPOAEs can be deduced from the fact that all these factors influence the amount of overlap between two excitation patterns in the cochlea and in turn determine the exact two-tone input to the nonlinear transduction of OHCs.

To date, all parametric studies on optimizing DPOAE recordings focus on the most prominent DP component, cubic difference tone (CDT, $2f_1 - f_2$). An obvious reason for CDT as the choice of DPOAE measure for research and application is simply its large size and SNR. Another reason is that at low signal levels CDT reflects the response growth or gain of OHC transducer and is parallel to hearing sensitivity and frequency selectivity of the inner ear (Brown *et al.*, 1993; Gorga *et al.*, 2003). However, CDT only represents the odd nonlinearity in cochlear transduction; thus, the estimation of hair cell function could not be complete without measuring the even-order DPs. The largest even-order DP is quadratic difference tone (QDT, $f_2 - f_1$) which has not been considered clinically useful until recently. One reason for the lack of research and application is due to its low amplitude (Brown, 1993) and poor SNR. However, auditory nerve fiber responses in kittens show robust QDT that can be larger than CDT (Tubach *et al.*, 1996). Neural QDT varies nonmonotonically with primary levels or frequencies and its behavior is different from CDT (Kim, 1980). Large QDT also presents in electrical responses in inner hair cells (Nuttall and Dolan, 1993), indicating that the source of QDT is presynaptic and possibly the OHCs. Indeed, QDT is the largest DP component found in the trans-membrane current that drives OHC somatic motility (Takahashi and Santos-Sacchi, 1999). Acoustic QDT can be associated with the saturating portions of OHC transduction, and its amplitude variation reflects the operating point (OP) shift of hair cells (Frank and Kössl, 1996). Studies in gerbils show that the QDT is enhanced or modulated by a low-frequency bias tone and the modulation patterns could be used to derive a cochlear transducer function ($F_{\mathrm{Tr}}$) (Bian, 2004, 2006). This finding poses a possible clinical application in evaluating cochlear function or diagnosing inner ear disorders. Since the cochlear $F_{\mathrm{Tr}}$ can be quantified from low-frequency modulation of CDT in humans (Bian and Scherrer, 2007), combining this measure with QDT could provide a more comprehensive picture of cochlear function. Towards this goal, it is necessary to explore the optimal signal conditions for recording QDT, because the ideal conditions for CDT may not be applicable to QDT, especially, in humans. Therefore, the purpose of the present study is to compare the optimal conditions for CDT and QDT to provide guidelines for research and clinical practice.

## II. METHODS

### A. Subjects

Sixteen healthy subjects with age ranging from 23 to 40 years (mean 26.3) were recruited from the students at Arizona State University (ASU). They had no history of hearing disorders. Normal outer and middle ear functions were confirmed with an otoscopic examination. A DP-gram was measured with an 8-point/oct procedure from 1 to 8 kHz (ILO92, Otodynamics Ltd., Herts, UK). Subjects with CDT amplitudes greater than 10 dB SPL in the frequency range between 1 and 4 kHz were selected for the study. Subjects with deep notches or spectral fine structures in this region were excluded to reduce interference of DPOAEs generated from reflections at the best frequency place (Knight and Kemp, 2001; Shera, 2004). To avoid possible influence and interference, the subjects were also screened to rule out spontaneous otoacoustic emissions in the testing ear. Subjects were seated comfortably in a soundproofed booth and instructed to be as quiet as possible during the test to reduce noises. The recruiting protocol and experimental procedures were approved by the Institutional Review Board of ASU.

### B. Stimulus presentation

Two primary tones were generated and controlled with a personal computer using software implemented in LABVIEW (National Instruments, NI, Austin, TX). Durations of the primary tones were 1 s with a 5-ms $\cos^2$-shaped rise and fall ramp, respectively. The signals were delivered separately to two earphones (ER-2A, Etymōtic Research, Inc., Elk Grove Village, IL) through a 24-bit dynamic signal acquisition and generation card (PXI-4461, NI) and acoustically mixed in the ear canal to stimulate the inner ear. The ear-canal acoustic response was then recorded by a calibrated probe microphone (ER-10B+). The recorded signal was amplified 20 dB by the built-in preamplifier of the ER-10B+ and digitized at a rate of 131.072 kS/s (PXI-4461). Prior to each test, the fit of ER-10B+ probe was checked and adjusted to ensure a flat ear-canal frequency response up to 5 kHz to a frequency-sweeping tone at a constant level. This can avoid the interference from standing waves in the ear canal and acoustic leaks around the probe.

Data were collected over a range of $f_2/f_1$ ratios using a "chess-grid" protocol, namely, the $L_1$ and $L_2$ were swept independently from 75 to 54 dB SPL in 3-dB steps to create an $8 \times 8$ grid of data sets for each $f_2/f_1$ ratio. Lower signal levels were not used due to a concern of poor SNR for QDT.

The primary levels were automatically adjusted and calibrated at the beginning of each decrement. To ensure the completion of experiments within 90 min, the frequency of $f_2$ was fixed at 4 kHz in the study. Based on the coverage of $f_2/f_1$ ratio, the study was carried out in two phases. In phase 1, the $f_2/f_1$ ratio was varied from 1.2 to 1.8 at a step size of 0.1 to explore the behaviors of CDT and QDT when $f_1$ and $f_2$ were separated further apart. It was initially thought that there could be a mechanical "(second) filter" just below the frequency of $f_2$ in the cochlea (Allen and Fahey, 1993; Brown *et al.*, 1993), so that the QDT could be "amplified" if the $f_2/f_1$ ratio was large enough to bring the QDT frequency into the filter bandwidth. In phase 2, conventional frequency ratios from 1.15 to 1.36 with a step size of 0.035 were used to reveal the optimal signal conditions for both DPOAE components. Ratios lower than 1.1 were not used to keep the QDT above 500 Hz, since the noise floor below this frequency was higher ($>-10$ dB SPL). Eight subjects participated in each phase.

### C. Data collection and analysis

At each two-tone condition, the stimuli were repeated eight times and the recorded acoustic signal was averaged in the time domain to reduce random noise. Noisy data due to body movements were discarded with an artifact rejection routine which examined the noise floor from 300 to 800 Hz. The rejection threshold was adjustable depending on the noise condition of each subject to optimize the speed of data collection. Data were analyzed offline in MATLAB (Mathworks Inc., Natick, MA) using custom-written programs. The waveform of ear-canal acoustic signal was passed through a Hanning window and converted into the frequency domain via a fast Fourier transform (FFT). Then, the spectral magnitudes at the frequencies of $2f_1-f_2$ and $f_2-f_1$ were extracted to result in the value of a single grid in the $L_1 \times L_2$ level space for CDT and QDT, respectively.

To examine the combined effects of primary levels and frequency ratio, the data were merged into an $8 \times 8$ grid of CDT or QDT amplitude-ratio functions with a specific $L_1$ and $L_2$ combination for each grid. Thus, the DPOAE amplitude could be examined in each dimension by fixing $L_1$, $L_2$, or $f_2/f_1$ ratio, respectively. For the optimal signal conditions, relations between the two primary levels under different frequency ratios or the optimal ratios as functions of the primary levels were inspected. As the influence of $L_1$ on DPOAE amplitudes was stronger than $L_2$, the relations among these signal variables were expressed as functions of $L_1$. To reveal possible underlying rules, these relations were fit with appropriate linear or nonlinear functions. The curve fittings were usually performed on the averaged data and the parameters were validated by predicting the optimal conditions for each individual.

## III. RESULTS

In this study, three signal variables, $L_1$, $L_2$, and $f_2/f_1$ ratio, were varied simultaneously, creating an extra complexity in observing the behaviors of DPOAEs. It would be convenient to reduce the data into a two- or three-dimensional space by keeping one variable constant. For the optimal signal conditions, the data analysis focused on the relations between these variables. Data reported were mostly from phase 2, where common $f_2/f_1$ ratios from 1.15 to 1.36 were used. Phase 1 data were reported in the section regarding the ratio effects.

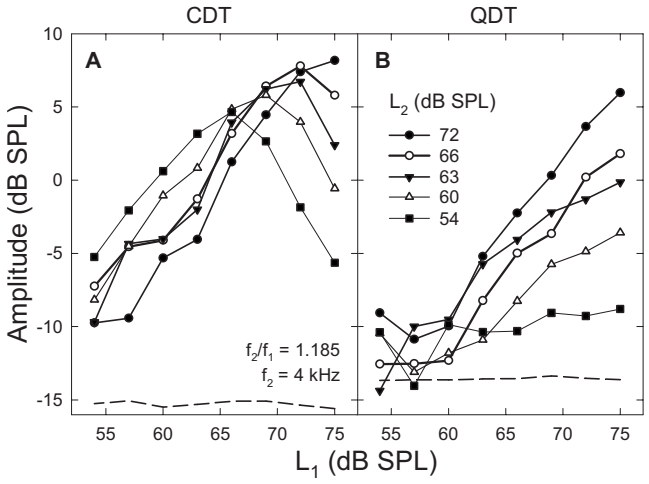


FIG. 1. DPOAE amplitudes as functions of $L_1$ under different $L_2$ settings. (A) CDT magnitudes rise with $L_1$ and roll over at different $L_1$ values. (B) QDT amplitudes increase with $L_1$ in different growth rates depending on the $L_2$ settings. Dashed lines indicate the averaged noise floor of DPOAE measures. Data reflect an average across eight subjects.

### A. Level effects

#### 1. $L_2$ fixed

For different $f_2/f_1$ ratios, the DPOAE magnitudes behaved similarly, but with different overall sizes. It would be reasonable to select a ratio that produced larger DPOAEs to show effects of $L_1$ when $L_2$ was fixed at different values. At the $f_2/f_1$ ratio of 1.185, amplitudes of CDT and QDT averaged across eight ears showed different growth patterns (Fig. 1) with $L_1$. The CDT amplitude showed an initial increase and a rollover as $L_1$ was raised over $L_2$ [panel (A)]. The level of $f_1$ where the CDT reached the peak depended on the fixed level of $f_2$, usually when $L_1$ was 3–10 dB greater than $L_2$. As the fixed $L_2$ decreased, the peaks of CDT amplitudes showed a small shift towards lower values of $L_1$, indicating a larger level difference. In other words, for lower levels of $f_2$ a much larger $L_1$ was needed to produce a peak CDT magnitude. Moreover, the peak CDT values decreased slightly ($<5-10$ dB) when $L_2$ was lowered for about 20 dB. Therefore, these CDT amplitude functions were largely overlapped when $L_1$ was below 65 dB SPL. The growth rates of CDT amplitudes were about 1 dB/dB, suggesting that the CDT increased proportionally with $L_1$ until the peak values were reached.

In contrast, the growths of QDT amplitudes showed no obvious signs of peaks and rollovers [Fig. 1(B)]. On average, the amplitudes of QDT were smaller than the CDT, especially, when $L_1$ was less than 60 dB SPL. At these lower $f_1$ levels, the QDT was usually within 5 dB from the noise floor (around $-12--13$ dB SPL). Then, the QDT amplitude started to grow when $L_1$ exceeded 60 dB SPL. The rate of

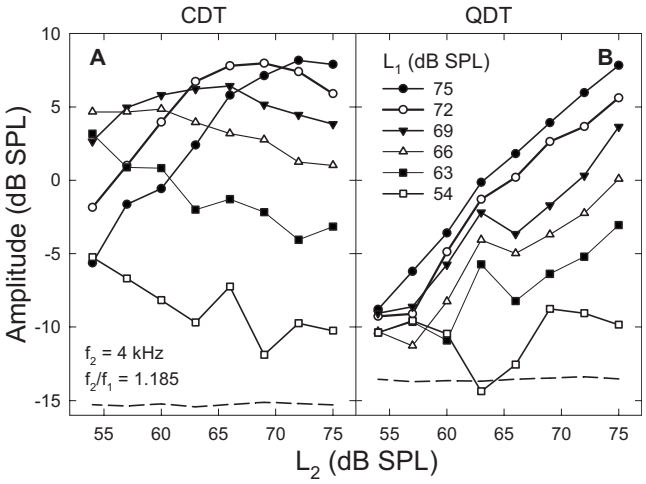


FIG. 2. DPOAE amplitudes as functions of $L_2$ under different $L_1$ settings. (A) CDT magnitudes show different patterns depending on the $L_1$ settings. The CDT peak decreases with $L_1$ and shifts to lower $L_2$ values as $L_1$ reduces. At lower $L_1$ settings, only a decrease in CDT level can be observed. (B) QDT amplitudes increase with $L_2$ in different growth rates depending on the $L_1$ settings. Note: a notch can be observed at moderate to low levels of the $f_1$. Dashed lines indicate the averaged noise floor of DPOAE measures. Data reflect an average across eight subjects.

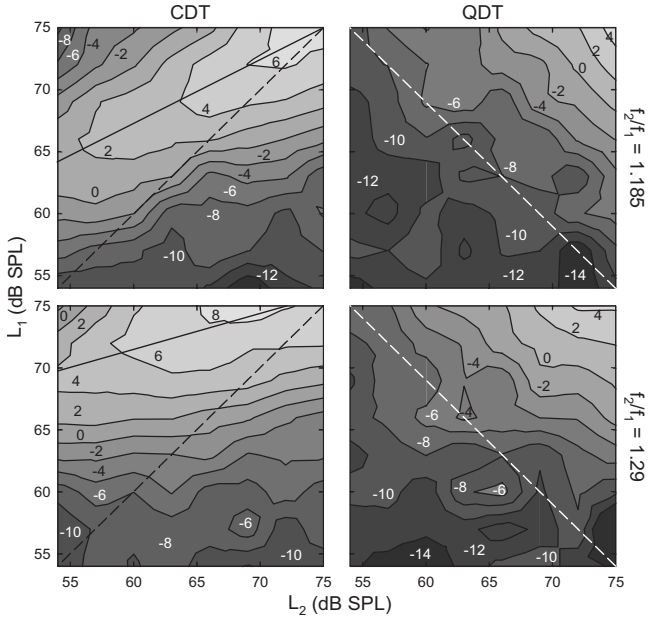


FIG. 3. Contour plots of DPOAE amplitudes in $L_1 \times L_2$ spaces of two $f_2/f_1$ ratios. Left: CDT magnitude shows a ridge spanning from the upper right corner (75,75) to moderate $L_1$ and low $L_2$. Solid lines indicate the optimal primary levels that yield the maximal CDT magnitude. Diagonal dashed lines indicate the condition $L_1=L_2$. Distances between the two lines represent the optimal level difference ($\Delta L=L_1-L_2$). Note: $\Delta L$ is greater for higher $f_2/f_1$ ratio (lower panel). Right: QDT magnitude contour lines are parallel to the diagonal dashed line representing $L_1+L_2=129$ dB SPL. For each fixed $L_1$ or $L_2$, maximizing the other primary level would optimize the QDT amplitude. Note: the slope of the contour for the larger ratio (lower panel) is shallower than the smaller ratio (top). Data reflect an average across eight subjects at an $f_2$ of 4 kHz.

growth and the maximal QDT level seemed to be proportional to the fixed level of $f_2$. The slope of QDT growth function could reach about 1 dB/dB when $L_2$ was set at 72 dB SPL and progressively decrease with $L_2$. QDT magnitudes usually reached their highest values when $L_1$ was maximal (75 dB SPL). The largest QDT level could be greater than 6 dB SPL when both $L_1$ and $L_2$ were at the highest level. There was also a slight compression of the QDT growth functions when $L_1$ was above 70 dB SPL.

### 2. $L_1$ fixed

When $L_1$ was fixed at different levels, the averaged CDT magnitude showed a range of different patterns as $L_2$ increased [Fig. 2(A)]. The patterns and overall value of CDT amplitudes were predominated by the fixed levels of $f_1$. As $L_1$ was gradually set to lower values, the CDT amplitudes showed three types of patterns with increasing $L_2$: (1) a compressive growth; (2) a slower initial growth with a rollover; and (3) a gradual decrease. The overall CDT magnitudes also decreased with reductions in $L_1$. The progression of these CDT patterns reflected a dramatic shift of the CDT peak towards lower $L_2$ along with a significant reduction in overall sizes. This indicated that CDT amplitudes could reach a higher value when $L_1$ was set higher and the CDT growth only occurred when $L_2$ was lower than $L_1$. Consistent with the growth curves in Fig. 1(A), the CDT peaked if $L_2$ reached 3–10 dB below the fixed $L_1$. When $L_2$ was greater than these levels or $L_1$, only a gradual decrease of CDT magnitude could be observed [Fig. 2(A)].

In comparison, the QDT amplitude showed a less variable growth pattern with the increase of $L_2$. When $L_1$ was fixed above 70 dB SPL, the QDT amplitude grew quite linearly with $L_2$. As $L_1$ was lowered, the growth functions of QDT became nonmonotonic with the presence of a notch around the $f_2$ levels of 63 to 67 dB SPL. There seemed to be a slight shift of the notch towards lower values of $L_2$. The QDT magnitude grew at a 1 dB/dB rate before the notch (lower $L_2$), which was consistent with the linear growths at high $f_1$ levels. If $L_1$ was very low (<55 dB SPL), the QDT level was flattened within about 5 dB from the noise floor (−13 dB SPL). Thus, QDT magnitudes were influenced by both $L_1$ and $L_2$.

### 3. Both $L_1$ and $L_2$ varied

The combined effects of $L_1$ and $L_2$ on the averaged CDT and QDT amplitudes were evaluated with contour plots in the $L_1 \times L_2$ level spaces (Fig. 3). From the DPOAE contours, the optimal signal levels that produced the highest DPOAEs could be evident. The CDT amplitude contour (left panels) showed a confined ridge spanning from the upper right corner towards the moderate values of $L_1$ and the minimal $L_2$. The tips of contour lines on the ridge, where both $L_1$ and $L_2$ were minimal to evoke a certain level of CDT, reflected the optimal primary levels for CDT. The relation between the optimal $L_1$ and $L_2$ (solid line) indicated that $L_1$ was preferred to be greater than $L_2$. This $\Delta L$ became progressively larger at lower primary levels with reference to the dashed line depicting $L_1=L_2$. At the $L_2$ of about 75 dB SPL, the optimal $L_1$ was roughly the same as $L_2$, i.e., no level difference. Comparing the contours from two different $f_2/f_1$ ratios (1.185 and 1.29), the optimal $\Delta L$ became larger for the higher frequency ratio (lower left panel). In addition, the CDT magnitude was

largely dominated by $L_1$ and the influence of $L_2$ was weak at higher ratios as indicated by the nearly horizontal contour lines.

Although the maximal QDT magnitudes were also located at the upper-right corners of the QDT contour maps (Fig. 3, right panels), paths of the isoamplitude lines were quite different from the CDT. These parallel contour lines stepped down towards lower $L_1$ and $L_2$ with no obvious ridges formed. The direction of the contour lines followed the diagonal line from the highest $L_1$ to the highest $L_2$ (dashed line), meaning that a relatively large QDT could be obtained by keeping one of the primary levels high. Thus, the QDT amplitude seemed to be proportional to $L_1+L_2$, i.e., higher QDT magnitudes correlated with larger sums of the primary levels. If one of the primary levels was fixed, raising the other could increase the QDT accordingly. This diagonal direction of contour lines was unaffected by varying the $f_2/f_1$ ratio. However, the contour gradient at the higher $f_2/f_1$ ratio (lower right panel) was shallower than the lower ratio (top right), indicating that larger QDT magnitudes could be observed at lower primary levels.

### B. Effects of the $f_2/f_1$ ratio

Since different ranges of $f_2/f_1$ ratios were adopted in phase 1 and phase 2 experiments, results from both phases were pooled together to evaluate the effects of a widely changed frequency ratio. Both CDT and QDT magnitudes showed a variability which was influenced by the amplitude and frequency of the emissions. The standard error (SE) of emission amplitudes was less than 2 dB when the emission magnitude was greater than −5 dB SPL or the frequency was above 1 kHz. The SE could increase up to 5 dB if the emission frequency and amplitude were below 500 Hz and −5 dB SPL, respectively. Despite the variability, the averaged DPOAE magnitudes showed different patterns as the $f_2/f_1$ ratio was increased from 1.15 to 1.8 (Fig. 4). As shown in this example ($L_1=L_2=72$ dB SPL), the CDT amplitude increased with the $f_2/f_1$ ratio starting from the lowest value of 1.15 and reached a maximum of nearly 8 dB SPL at the ratios of 1.22 to 1.25. Then, the CDT magnitude decreased quickly as the ratio further increased and dropped below −5 dB SPL for the ratios above 1.4. The QDT magnitude, however, showed an opposite change when the $f_2/f_1$ ratios were below 1.4, i.e., it produced a notch with a minimum of −2 dB SPL at the ratio of about 1.25. With further increase in the ratio, QDT levels bounced back and reached a peak at 1.36. For $f_2/f_1$ ratios greater than 1.4, both CDT and QDT magnitudes reduced continuously. Despite a slower reduction, the QDT amplitude showed no signs of a bandpass characteristic ("the second filter") when the $f_2/f_1$ ratio increased to 1.8, a ratio where the QDT frequency was equivalent to the CDT generated at the ratio of 1.36. From the CDT curve, a dramatic 10-dB increase in amplitude could be observed from the ratios of 1.4 to 1.32.

The opposite behaviors of CDT and QDT were also presented under the conditions of unequal primary levels. A series of averaged CDT and QDT amplitude-ratio functions was displayed to examine the influence of $L_1$ with $L_2$ held

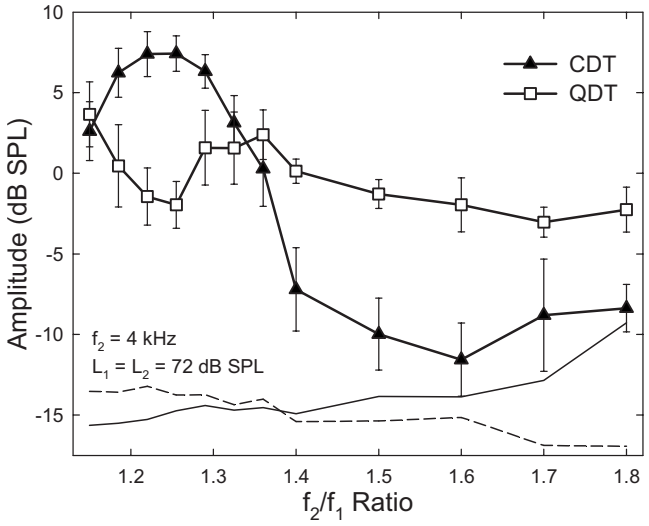


FIG. 4. DPOAE amplitudes as functions of $f_2/f_1$ ratio. Each curve is a combination of the averaged results from the two experimental phases. For frequency ratios below 1.4, the CDT amplitude reaches a peak at about 1.25, where the QDT magnitude drops to a local minimum. For $f_2/f_1$ ratios above 1.4, both CDT and QDT amplitudes decline to minimal values at the frequency ratios of 1.6 and 1.7. Error bars represent the standard errors of the data. Solid and dashed lines indicate the averaged noise floor in CDT and QDT measures, respectively. Each data point reflects an average across eight subjects.

constant at 72 dB SPL (Fig. 5). It could be observed from panel (A) that the CDT amplitudes showed an asymmetrical bell shape as the frequency ratio varied. The peaks of CDT curves progressively shifted towards lower ratios when $L_1$ decreased, i.e., the optimal $f_2/f_1$ ratio for CDT was smaller (<1.2) for lower $f_1$ levels (<66 dB SPL). For QDT magnitudes [panel (B)], a notch presented at about 1.22–1.25 for different levels of $f_1$. However, no clear trend of shifting of the notch could be observed. On either side of the notches, the QDT level peaked around the frequency ratios of 1.18

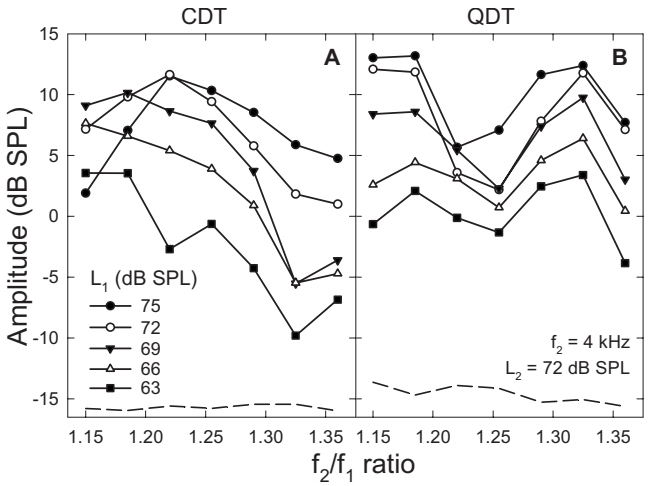


FIG. 5. Effects of primary levels on DPOAE amplitude-ratio functions. (A) As $L_1$ decreases, the peak of CDT amplitude shifts to lower $f_2/f_1$ ratios. (B) QDT magnitudes show a notch around the $f_2/f_1$ ratios of 1.22–1.25. No obvious shift of the notches can be observed with varying $L_1$. Among the two possible optimal ratios (1.185 and 1.325), the larger one is selected as the optimal ratio for recording QDT so that the QDT frequency can be maintained above 500 Hz. Data reflect an average across eight subjects.

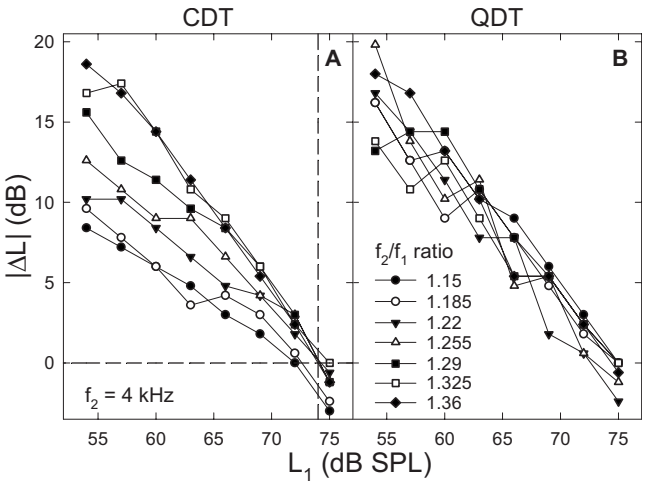


FIG. 6. Effect of $L_1$ on the optimal primary $\Delta L$. For both CDT and QDT, the optimal $\Delta L$ declines with the increase in $L_1$. Different lines represent different $f_2/f_1$ ratios in each panel. (A) The slope of $\Delta L$ decrease with $L_1$ varies depending on the $f_2/f_1$ ratio. The maximal $\Delta L$ at the lowest $L_1$ is proportional to the frequency ratio and $\Delta L$ approaches zero around the $L_1$ of 74 dB SPL (dashed lines). (B) Similar trends can be observed in the $\Delta L$ for measuring QDT, but the effect of $f_2/f_1$ ratio is minimal. Note: the absolute value of $\Delta L$ is used, i.e., $|\Delta L|=L_1-L_2$, because $L_2$ could be greater than $L_1$ for recording QDT. Data reflect an average of eight subjects.

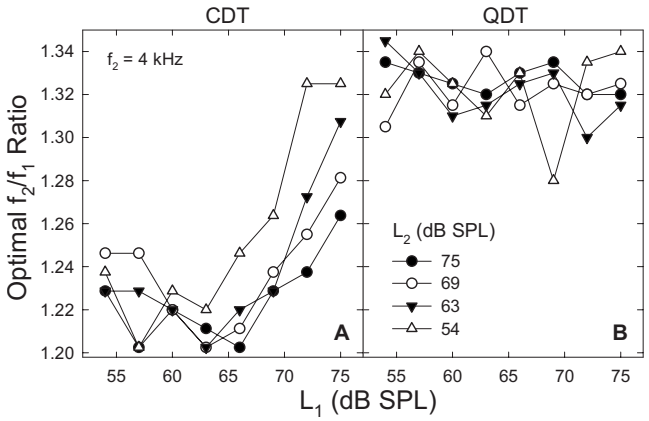


FIG. 7. Influence of primary levels on optimal $f_2/f_1$ ratio. (A) After an initial dip, the optimal frequency ratio increases nonlinearly with $L_1$. The rate of $f_2/f_1$ growth and the maximal value are inversely related to $L_2$. The minimal ratios ($>1.20$) present at the $L_1$ of about 55–65 dB SPL. (B) The optimal $f_2/f_1$ ratios for QDT vary between 1.3 and 1.34 with only a slight decrease with $L_1$. No influence from $L_2$ can be observed. Data reflect an average of eight subjects.

and 1.32, respectively. For levels of $f_1$ below 70 dB SPL, the patterns of QDT amplitude were more asymmetrical, with peaks at the ratio of 1.32 being higher.

### C. Optimal signal conditions

#### 1. Primary level difference

Inter-relations among the optimal signal conditions ($L_1$, $L_2$, and $f_2/f_1$ ratio) were explored and quantified. As noted above, $L_1$ should be greater than $L_2$ to evoke a large CDT (Fig. 3 left) and the $\Delta L$ was greater at lower primary levels. The $\Delta L$ was further affected by the $f_2/f_1$ ratio, i.e., larger for higher ratios, and the optimal ratio increased with the primary level [Fig. 5(A)]. These relations were depicted with a series of optimal $\Delta L$s obtained at different frequency ratios plotted as functions of $L_1$ (Fig. 6). For CDT [panel (A)], these $\Delta L$s decreased linearly with the $L_1$ and became 0 at the $L_1$ of about 74 dB SPL. The only obvious difference among these $\Delta L$ functions was their varying slopes that decreased with the $f_2/f_1$ ratio. Thus, the $\Delta L$ functions could be fit with a cluster of straight lines passing through a single point (74, 0),

$$\Delta L = K(r)(L_1 - 74), \tag{1}$$

where $K(r)$ is the slope of the $\Delta L$ functions. Note that the slope $K$ is a function of the $f_2/f_1$ ratio ($r$) and the values are listed in Table I. As can be observed, the relation between the slopes and the ratios was approximately linear with a 0.96 correlation coefficient ($r^2$). Therefore, the slope could be obtained from $K(r)=a\cdot r+b$, where $a=-2.09$, $b=1.91$.

For QDT, $\Delta L$ was also reduced as $L_1$ increased [Fig. 6(B)]. Unlike CDT, these $\Delta L$ functions for different $f_2/f_1$ ratios were close to each other, indicating that the influence of the frequency ratio was weak. The slopes of these $\Delta L$ functions were approximately $-1$, meaning that the effect of primary levels was a linear decrease with increasing $f_2/f_1$ ratio. Solving Eq. (1) with $K=-1$, there were two possible relations between the primary levels: one of the primaries $L_1$ or $L_2=74$ dB SPL, or $L_1=L_2/2+37$, if both primaries were at moderate levels. However, the second solution was not the optimal condition, because for a given primary level the sum of $L_1$ and $L_2$ was not greater than when the other tone was held at the maximal value. It should be noted that $L_2$ could be greater than $L_1$ to evoke a large QDT.

#### 2. Frequency ratio

For CDT, the influence of primary levels on the optimal $f_2/f_1$ ratio was mainly from $L_1$, since the ratio showed only a small reduction with $L_2$ (data not shown). At different $L_2$ levels, the optimal ratio as functions of $L_1$ demonstrated a series of "$J$"-shaped curves [Fig. 7(A)]. Generally, the optimal ratio declined slightly as $L_1$ increased to 60–65 dB SPL. With further increase in $L_1$, the ratio rose considerably. As $L_2$ was lowered, the optimal ratio change with $L_1$ showed three trends: (1) a steeper slope; (2) a higher maximal ratio; and (3) a shift of the minimum to lower $L_1$. For each fixed $L_2$, the ratio curve could be fit with a quadratic function,

TABLE I. Relation between the $f_2/f_1$ ratio ($r$) and the slope $K$ used for calculating the primary level difference ($\Delta L$) in Eq. (1).

| $r$ | 1.15 | 1.185 | 1.22 | 1.255 | 1.29 | 1.325 | 1.36 |
|---|---|---|---|---|---|---|---|
| $K$ | −0.52 | −0.56 | −0.64 | −0.66 | −0.78 | −0.90 | −0.93 |

TABLE II. Relation between $L_2$ and the parameters in Eq. (2). $r^2$: correlation coefficient of a linear regression between the parameter and the $L_2$.

| $L_2$ (dB SPL) | 75 | 72 | 69 | 66 | 63 | 60 | 57 | 54 | $r^2$ |
|---|---|---|---|---|---|---|---|---|---|
| $r_0$ | 1.223 | 1.227 | 1.230 | 1.230 | 1.224 | 1.233 | 1.236 | 1.228 | 0.62 |
| $s(\times 10^{-4})$ | 2.31 | 1.72 | 2.65 | 1.75 | 5.52 | 4.53 | 4.33 | 5.06 | 0.74 |
| $L_0$ (dB SPL) | 65.44 | 64.96 | 63.9 | 61.61 | 63.98 | 62.20 | 61.91 | 61.15 | 0.37 |

$$r = r_0 + s(L_1 - L_0)^2, \tag{2}$$

where $r_0$ is the minimal $f_2/f_1$ ratio (when $L_1=L_0$) and $s$ is the slope of ratio growth. Values of the parameters obtained from curve fitting varied with $L_2$ (Table II). For simplicity, linear functions were used to approximate the relations between the parameters and $L_2$,

$$\begin{cases} r_0 = c_1 L_2 + d_1 \\ s = c_2 L_2 + d_2 \\ L_0 = c_3 L_2 + d_3 \end{cases}, \tag{3}$$

where $c_1=-3.65\times10^{-4}$, $d_1=1.25$, $c_2=-1.65\times10^{-5}$, $d_2=1.42\times10^{-3}$, $c_3=0.19$, and $d_3=50.91$.

There could be two optimal ratios for QDT as indicated by the two peaks of the QDT amplitude-ratio patterns [Figs. 4 and 5(B)]. Only the larger ratio was chosen to keep the QDT frequency above 500 Hz for a better SNR. For QDT, no systematic increase of the optimal $f_2/f_1$ ratio was observed [Fig. 7(B)]. The ratios fluctuated between 1.30 and 1.34 regardless of $L_2$. Examined across different levels of $L_2$, the frequency ratios showed a slight decrease with increasing $L_1$. On average, the $f_2/f_1$ ratios ranged from 1.32 to 1.33. Therefore, the influence of primary levels on the $f_2/f_1$ ratio to record QDT was weak and a value slightly greater than 1.3 could be used as the optimal frequency ratio.

## IV. DISCUSSION

To explain the experimental results and explore the generating mechanisms of DPOAEs, a model combining the cochlear mechanics of traveling wave and the nonlinearity in hair cell transduction is used (Fig. 8). Simulated effects of manipulating the primary tones are compared with experimental data. Adding a traveling-wave component to the hair cell transducer model (Bian *et al.*, 2002) is to determine the extent of two-tone interaction on the basilar membrane (BM) and the exact input levels to hair cell transduction.

### A. Interaction of traveling waves

A simplified gamma-tone envelope (Carney, 1993) can be used to describe the spread of excitation or displacement along the BM in response to a pure tone,

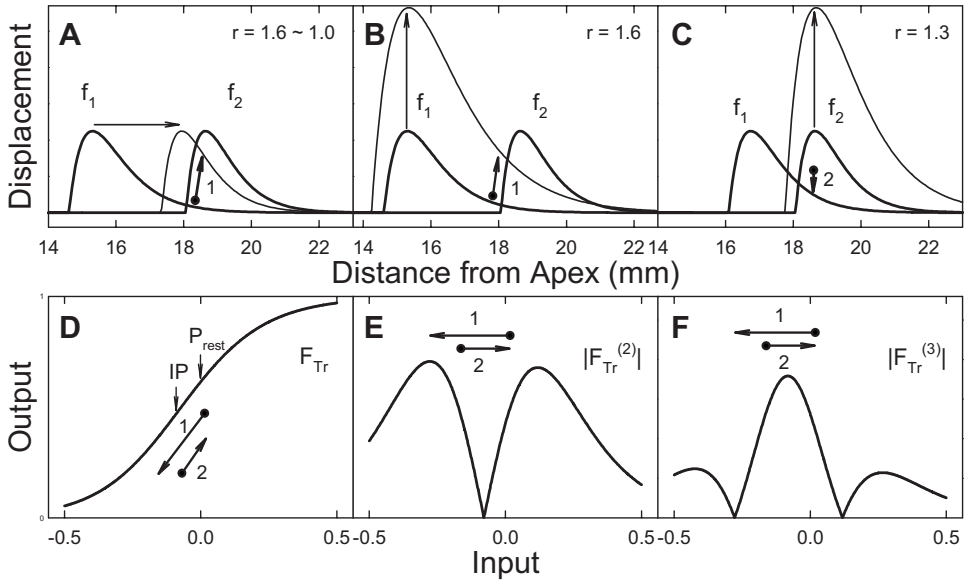


FIG. 8. A model of DPOAE generation. Top row: two tone interaction via traveling waves. (A) Sweeping $f_1$ to reduce the $f_2/f_1$ ratio ($r$) while keeping primary levels constant ($L_1=L_2$). (B) Increasing $L_1$ while keeping the $f_2/f_1$ ratio constant. The overlap of traveling wave envelopes increases as $f_1$ approaches $f_2$ or as $L_1$ increases. Influence of $f_1$ on $f_2$ or the effective $L_1$, as indicated by the crossing point of the envelopes, rises accordingly. The direction of the crossing point change (dot arrow) marks the direction of OP shift on the $F_{Tr}$ (path 1). (C) Raising $L_2$ while keeping the frequency ratio constant. As $L_2$ increases, changes in the overlapped region and the effective $L_1$ are small. Actually, the influence of $f_1$ on $f_2$ is reduced. Relative to the $f_2$ peak, the direction of the crossing point change (dot arrow) is reversed (path 2). Bottom row: the hair cell transducer nonlinearity and DP generation. The direction and path of the OP shift resulting from traveling wave interactions are indicated by the numbered dot arrows. (D) A cochlear $F_{Tr}$ marked with the resting position ($P_{rest}$) and inflection point (IP). (E) and (F) Absolute values of the second and third derivatives of the $F_{Tr}$, or $|F_{Tr}^{(2)}|$ and $|F_{Tr}^{(3)}|$, respectively. Following the OP paths, the differential behaviors of QDT and CDT can be observed from panels (E) and (F).

$$P_{\mathrm{TW}}(l) = n \cdot l \cdot e^{-nl}, \tag{4}$$

where $P_{\mathrm{TW}}$ is the traveling wave envelope as a function of the BM location $l$ in millimeters from the apex and $n$ is a constant which is unique to the traveling wave peak location ($l_{\mathrm{P}}$). Since the slope or derivative of the envelope at its peak is zero, i.e., $P'_{\mathrm{TW}} = n(1-nl)e^{-nl} = 0$, thus $n = 1/l_{\mathrm{P}}$. Ideally, $l_{\mathrm{P}}$ is determined by the cochlear frequency map (Greenwood, 1990), where the characteristic frequency ($f_{\mathrm{CF}}$) location from the apex is $l_{\mathrm{CF}} = (1/\alpha)\log_{10}(f_{\mathrm{CF}}/A + k)$, where $\alpha = 0.06$ mm$^{-1}$, $A = 165$ Hz, and $k = 1$ for humans. With increasing stimulus level, two alterations in traveling wave properties are also implemented: a basal peak shift and an envelope widening. Since the maximal peak shift is about 1/2 octave above the $f_{\mathrm{CF}}$ (Robles and Ruggero, 2001), the shift can be quantified as $l_{\mathrm{P}} = l_{\mathrm{CF}} + (l_{1.5\mathrm{CF}} - l_{\mathrm{CF}})L$, where $L$ is the signal level in pascals. Width of the traveling wave is defined as the distance between $l_{\mathrm{P}}$ and the apical zero crossing ($l_0$). Given a 35-mm-long BM, the width is a fraction ($w$) of the basal portion of the traveling wave ($35 - l_{\mathrm{P}}$). This yields to $l_0 = l_{\mathrm{P}} - w(35 - l_{\mathrm{P}})L^{1/2}$, where $w = 1/3$. Thus, the actual traveling wave envelope is calculated as

$$P_{TW}(l) = \begin{cases} n(l - l_0)e^{-n(l-l_0)} \\ 0, \quad \text{if } l < l_0, \end{cases} \tag{5}$$

where $n = 1/(l_{\mathrm{P}} - l_0)$ and the BM apical to $l_0$ does not respond.

Since DPs are generated from the overlapped region of two traveling wave envelopes initiated by the primary tones [Fig. 8(A)], only a portion of the $f_1$ envelope contributes to the two-tone interaction. The effective $L_1$, indicated by the crossing point of $f_1$ and $f_2$ envelopes, is critical in determining the contribution of $f_1$ and the influence of $f_1$ on $f_2$ (Lukashkin and Russell, 2001). Effects of $f_1$ with respect to a fixed $f_2$ were systematically examined by: (1) varying $f_1$ with equal primary levels; (2) varying $L_1$ with $f_1$ fixed; and (3) varying $L_2$ with a fixed $f_2/f_1$ ratio [Figs. 8(A)–8(C)]. As $f_1$ approaches $f_2$ [panel (A)], the overlapped region becomes larger and the effective $L_1$ at the crossing point climbs up. When both $f_1$ and $f_2$ are fixed, increasing $L_1$ enlarges the traveling wave overlap and the effective $L_1$ (panel B), similar to raising $f_1$. The manipulation of $L_2$, however, produces a limited effect, because the basal slope of $f_1$ envelope is shallow and expansion of apical portion of $f_2$ pattern is small [Fig. 8(C)]. All three situations produce more or less similar changes of the CDT, i.e., a limited or saturated increase in CDT amplitude, since the effective $L_1$ is limited by the $f_2/f_1$ ratio of 1, or the fixed settings of $L_2$ and $L_1$. Increase in traveling wave overlap alone cannot explain the nonmonotonic changes in DPOAE magnitudes and differential behaviors of CDT and QDT (Figs. 1–5). In essence, the optimal signal conditions are not solely dependent on traveling wave interactions. A second component in the model, the transducer nonlinearity, is thus necessary.

### B. Interaction with the hair cell transducer

The nonlinearity of OHC transducer is characterized by a second-order Boltzmann function [Fig. 8(D)] relating cochlear responses to the BM displacement $x$ (Bian *et al.*, 2002),

$$F_{\mathrm{Tr}} = F_{\max}/[1 + e^{bx-c}(1 + e^{dx-e})], \tag{6}$$

where $F_{\max}$ is a scaling factor determining the maximal output, $(b,d)$ are slope constants, $(c,e)$ are constants setting the resting position of the hair cell transducer. The main advantage of using the second-order Boltzmann function is its asymmetry. The inflection point (IP) on the $F_{\mathrm{Tr}}$ curve is located off zero input (resting point) and the slopes on two sides are different (Bian, 2004). These $F_{\mathrm{Tr}}$ asymmetries can be observed from the center notch or peak of the absolute values of its second and third derivatives (corresponding to the IP) and the sizes of sidelobes [panels (E) and (F)]. Note that there is a 180° phase difference between the sidelobes or side and center peak of the second and third derivatives, respectively. In addition to traveling wave interactions, the second and third derivatives of $F_{\mathrm{Tr}}$ largely dictate the behaviors of QDT and CDT.

#### *1. Ratio effects*

Influence of $L_1$ on the overlapped region is not only a modification of actual input to the cochlear transducer, but also a biasing of the OP of hair cells in that region due to a tilting of hair bundles or shrinking of cell bodies caused by the $f_1$ traveling wave. With the absence of $f_1$ or when $f_1$ is far away from $f_2$, the OP at the $f_2$ place usually is at the resting point [Fig. 8(D)]. When $f_1$ approaches $f_2$, or $L_1$ steps up, the BM may undergo a progressive baseline shift or an OP shift [Figs. 8(A) and 8(B)]. The direction of OP shift on $F_{\mathrm{Tr}}$ could be from the resting position towards the IP (path 1). When the influence of $f_1$ becomes very large, e.g., at a very small $f_2/f_1$ ratio or an intense $L_1$, the OP could pass the IP and eventually approach the minima on the third derivative [panel (F)]. Therefore, the CDT magnitudes, as functions of $f_2/f_1$ ratio [Figs. 4 and 5(A)] or $L_1$ [Fig. 1(A)], show a maximum and a rollover. Another evidence for the OP shift across the IP could be the notch presented on the QDT amplitude-ratio functions [Figs. 4 and 5(B)], which was also observed by Brown (1993). The simulated results of QDT and CDT (Fig. 9) well represent the scenarios of OP shifts on the second and third derivatives of $F_{\mathrm{Tr}}$ as the $f_2/f_1$ ratio is reduced.

A result of the simulation is that the CDT magnitudes reach a minimum and then increase when the $f_2/f_1$ ratio is reduced below about 1.1 [Fig. 9(A)]. This notch could not be observed in the present study due to the limited frequency ratio selection ($\geq 1.15$). However, the notch in CDT amplitude-ratio function has been reported in adults (Harris *et al.*, 1989, Moulin, 2000; Londero *et al.*, 2002) and neonates (Abdala, 1996; Lasky, 1997; Vento *et al.*, 2004). Applying the above scenario and following path 1 of the OP shift, the CDT can reach a minimum and regain its magnitude when $f_1$ further approaches $f_2$ [Fig. 8(F)]. It has been suggested that when $f_2/f_1 < 1.1$, reflection or place-fixed

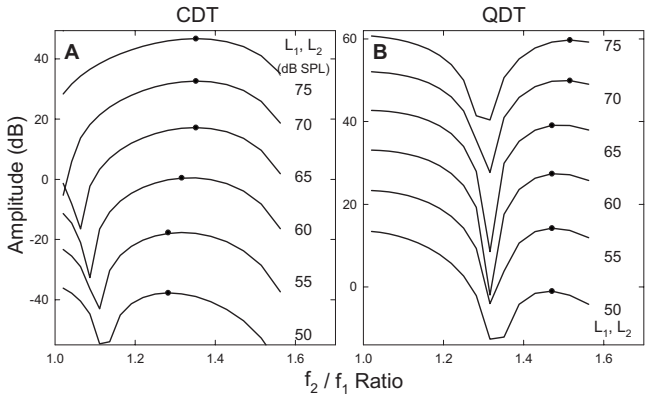


FIG. 9. Model simulation: effects of $f_2/f_1$ ratio. (A) CDT magnitudes are maximized at the ratio between 1.2 and 1.3 and otherwise reduced. The peak CDT amplitude (dots) shifts to higher ratios with increase in primary levels ($L_1$=$L_2$). Note: a notch is presented at the $f_2/f_1$ ratio of about 1.1. (B) QDT amplitudes are minimized at the frequency ratio of about 1.3 and maximized at higher (>1.4) or lower ratios. The maximal QDT magnitudes at the higher ratios are marked with dots.

DPOAEs may become dominant (Stover *et al.*, 1999; Knight and Kemp, 2001; Dhar *et al.*, 2005) and cancel the nonlinearly generated DPs. However, the possibility that a nonlinear mechanism alone is capable of producing the notch cannot be ruled out (Lukashkin and Russell, 2001). Several investigators have measured the widths of CDT amplitude-ratio functions as the bandwidth of a "second cochlear filter" (Brown *et al.*, 1993; Abdala, 1996; Vento *et al.*, 2004) and found it narrower at lower primary levels. The simulated results [Fig. 9(A)] are consistent with these observations. Although the "second filter" is not evident by bringing the QDT frequency into the filter bandwidth (Fig. 4; Fahey *et al.*, 2006), the shape of CDT amplitude-ratio function partly reflects the third derivative of cochlear $F_{Tr}$ which is level dependent (Patuzzi and Moleirinho, 1998; Bian and Chertoff, 2001). Indeed, the sharpness of cochlear filter and the hair cell transducer gain may be intimately related.

### *2. Level effects*

The effect of increasing $L_1$ is similar to reducing $f_2/f_1$ ratio where the CDT amplitude first increases and then rolls over [Fig. 1(A)]. The nearly linear growth of CDT with $L_1$, which is also observed by others (Gaskill and Brown, 1990; Whitehead *et al.*, 1995; Dreisbach and Siegel, 2005), may reflect the elevation of the effective $L_1$ at the overlap of traveling wave envelopes [Fig. 8(B)]. Since the apical slope of $f_2$ traveling wave envelope is very steep, the increase of effective $L_1$ follows the rise of the tail of $f_1$ envelope proportionally. When $L_1$ exceeds $L_2$, the traveling wave overlap reaches a maximum and the OP may shift (path 1) to the IP of $F_{Tr}$, thus producing a peak in CDT magnitude. Unlike the frequency ratio change, the CDT-$L_1$ functions rarely show a notch [Fig. 1(A)]. However, such a notch is frequently found in gerbils (Mills, 2002) and chinchillas (Rhode, 2007), because the frequency places of the primaries are closer in small rodents and $L_1$ is perhaps more effective in biasing OHCs at the $f_2$ place. At the lowest $f_2/f_1$ ratio (1.15), a notch was indeed observed on the $L_1$ side of the $L_1 \times L_2$ space. It is worth noting that larger $f_2/f_1$ ratios are used to evoke DPOAEs in rodents (Brown, 1987).

In contrast, increasing $L_2$ may result in an opposite OP shift, because the influence of $f_1$ on $f_2$ diminishes as $L_2$ rises due to unchanged effective $L_1$ [Fig. 8(C)]. The direction of OP shift is from a prebiased position in the negative pressures towards the resting position of hair cell $F_{Tr}$ (path 2). Depending on the value of $L_1$, the initial OP shift could vary, thus resulting in variable patterns of CDT amplitude [Fig. 2(A)]. For high $f_1$ levels, the initial OP shift is large and the OP can pass through the IP as $L_2$ increases, causing CDT to rise and fall [Fig. 8(E)]. For lower $L_1$, the small initial shift may not even reach the IP, and CDT can only show a decrease as the OP returns to its resting point. These different patterns are indeed observed as increasing $L_2$ while holding $L_1$ at various levels [Fig. 2(A); Hauser and Probst, 1991]. Notches of the QDT amplitude in Fig. 2(B) may also indicate the OP path. However, the OP shift on QDT is less influential than the primary levels. This can be evident from the QDT contours in humans (Fig. 3, right) and rabbits (Martin *et al.*, 2003) that show diagonal contour lines indicating increasing influences from both primary levels. In contrast, the ridge on CDT contours implies that a specific influence of $L_1$ on $L_2$, i.e., a unique OP shift, can maximize the amplitude. From Figs. 8(D)–8(F), it can be noted that CDT at lower input level is related to the center peak of the third derivative and the IP. In contrast, QDT is associated with sidelobes of the second derivative that are maximal for high input levels or large OP shifts. Moreover, sidelobes of the second and third derivatives are both related to saturation regions of the $F_{Tr}$. Indeed, the direction of QDT contour line is consistent with the "passive" CDT evoked at high primary levels (Mills, 1997).

## C. Optimal signal conditions

Descriptions of the optimal signal conditions derived from the simulation are comparable with the experimental results. For equal primary levels, the optimal frequency ratio for CDT increases with the signal level [Fig. 9(A)], which is consistent with the observations in the present study (Figs. 4 and 5) and works by others (e.g., Johnson *et al.*, 2006). The level-dependent drift of the optimal ratio is probably due to narrower traveling wave envelopes at low levels so that the two tones need to be placed closer to produce an interaction. Unlike the CDT, the optimal ratio for QDT shows no obvious drift with the primary level [Figs. 5(B) and 9(B)]. One reason for this difference could be that the deep notch on the second derivative of $F_{Tr}$ [Fig. 8(E)] could severely affect the QDT magnitude compared to variations in traveling wave overlap.

Another important signal parameter is $\Delta L$, which shows two linear relations in both experimental and simulated results (Figs. 6 and 10). First, $\Delta L$ decreases linearly with $L_1$. Such a linear decrease is predictable from the differential growths of BM vibrations at the $f_2$ place in response to $f_1$ and $f_2$ (Kummer *et al.*, 2000), i.e., linear growth of effective $L_1$ and compression of $L_2$. Additional sound pressure is re-

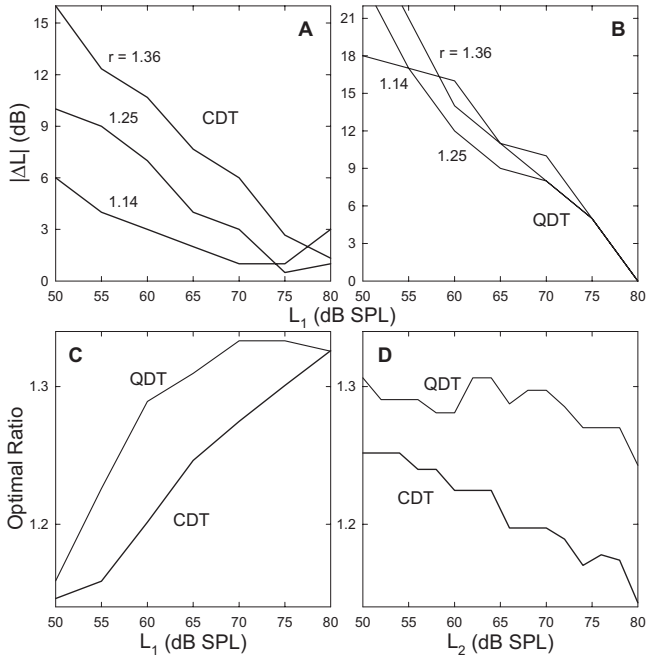


FIG. 10. Model simulation: optimal signal conditions. (A), (B) Influence of $L_1$ on primary $\Delta L$. For both CDT and QDT, the $\Delta L$ decreases with $L_1$. For CDT, the slope of the $\Delta L$ decrease is proportional to the $f_2/f_1$ ratio; however, such an effect is minimal for QDT. (C), (D) Effects of the primary levels on the optimal frequency ratio. For both CDT and QDT, the ratio increases with $L_1$ and slightly reduces with $L_2$. These level effects are smaller for QDT. Note the optimal frequency ratio is higher for QDT than CDT.

quired to compensate the insensitivity for $f_1$ at the $f_2$ location until about 70–75 dB SPL, where tuning at the $f_2$ place is broadened. Second, for CDT, the slope of $\Delta L$ decrease is proportional to the $f_2/f_1$ ratio [Figs. 6(A) and 10(A)]. Again, it becomes clear that the tuning property at the $f_2$ place determines that a smaller $\Delta L$ is required for a more closely placed $f_1$ to produce a certain level of interaction [Figs. 8(A)–8(C)]. These linear trends allow the derivation of Eq. (1) to calculate the ultimate $\Delta L$ for a given frequency ratio. Other formulas (Whitehead *et al.*, 1995; Kummer *et al.*, 2000) are also developed in a similar way. A formula by Johnson *et al.* (2006), incorporates the $f_2$ and can be applied to different frequencies. Our formula in Eq. (1), however, includes the $f_2/f_1$ ratio and is flexible for situations where the ratio is predetermined.

In practice, $f_2$ and $L_2$ are usually preselected to assess cochlear functions at a particular frequency location. The decisions to be made are to find $f_1$ by selecting an appropriate $f_2/f_1$ ratio and to determine $L_1$. From the experimental data and model simulation, it is known that the optimal $f_2/f_1$ ratio is nonlinearly dependent on the primary level [Figs. 7, 10(C), and 10(D)]. For CDT, the optimal ratio stays low for lower values of $L_1$ and grows quickly at higher levels. The quadratic fit of the optimal ratio function coincides with the formula of Johnson *et al.* (2006), in which a squared $L_2$ is used. The effect of $L_2$ on the optimal frequency ratio is a slight decrease [Fig. 10(D)]. Moving $f_1$ closer could produce more two tone interactions if $L_2$ is substantial, whereas moving $f_1$ away could avoid suppressing $f_2$ if $L_2$ is weak. For QDT, the simulated optimal ratios (about 1.3) are generally comparable with the data for $L_1 > 65$ dB SPL [Figs. 7(B) and 10(D)], even though the measured ratios show no obvious change with the primary levels.

For CDT, the complex interactions among frequency ratio and primary levels could be determined from the abstracted relations between a collective pairs of variables. Therefore, two of the relations are formulated using $\Delta L$ and optimal ratio [Eqs. (1) and (2)]. Since these relations coexist, the optimal conditions should satisfy both equations. Therefore, a set of two formulas is proposed for obtaining the optimal signal conditions for CDT,

$$\begin{cases} [1-(a\cdot r+b)]L_1 = L_2 - 74(a\cdot r+b) \\ r = r_0 + s(L_1 - L_0)^2 \end{cases}, \tag{7}$$

where $r_0 = c_1 L_2 + d_1$, $s = c_2 L_2 + d_2$, and $L_0 = c_3 L_2 + d_3$. Solving both equations together, the optimal $f_1$ and $L_1$ could be determined. These formulas with parameters obtained from the data predict the optimal conditions for each subject in the study. Using $f_2/f_1$ ratio as an example, the prediction accuracy is as high as 95% with an average of 73%. From Eq. (7), the calculated values of $L_1$ and $f_2/f_1$ are well comparable with results in humans (Kummer *et al.*, 2000; Johnson *et al.*, 2006) and rodents (Pibal *et al.*, 2002; Michaelis *et al.*, 2004). Parameters used in the formulas still need to be tested and refined by large-scaled studies with wider stimulus ranges.

## V. SUMMARY AND CONCLUSION

Amplitudes of CDT and QDT were measured within a finite $L_1 \times L_2$ space across a wide range of $f_2/f_1$ ratios. For CDT, three relations are found among the optimal signal conditions: (1) $L_1$ should always be greater than $L_2$, until about 74 dB SPL where the level difference diminishes; (2) the rate of primary $\Delta L$ decrease is proportional to the $f_2/f_1$ ratio; and (3) the optimal frequency ratio increases with $L_1$ in a nonlinear fashion. A set of two formulas is proposed to quantify the optimal signal conditions, namely, $f_1$ and $L_1$ for a given $L_2$. For QDT, different relations are observed: (1) maximizing one of the primary levels can optimize the QDT amplitude; (2) the $\Delta L$ decreases with the signal level, but independent of the $f_2/f_1$ ratio; and (3) the optimal frequency ratio was constant at just over 1.3. An important finding is the QDT notch around the optimal ratio for CDT (1.22–1.25). Therefore, the optimal signal conditions for CDT cannot be applied to QDT. If applied cautiously to avoid system distortions, maximizing the signal level could allow for recording of robust QDT and CDT that may persistent after cochlear damages (Avan *et al.*, 2003). The present results are consistent with the notion that DPOAEs mainly originate from the OHC nonlinearity in the overlapped region of the traveling waves. Optimizing DPOAE recordings could improve the measurement reliability and repeatability, thus allowing for more accurate estimates of cochlear function and a wider range of clinical utilities.

## ACKNOWLEDGMENTS

We thank the subjects for their patience and Tina Stinson for recruiting some of the participants. This work was supported by a grant (R03 DC006165) from the National Insti-

tute on Deafness and Other Communication Disorders of the National Institutes of Health.


Abdala, C. (**1996**). "Distortion product otoacoustic emission ($2f_1-2f_2$) amplitude as a function of $f_2/f_1$ frequency ratio and primary tone level separation in human adults and neonates," J. Acoust. Soc. Am. **100**, 3726–3740.

Allen, J. B., and Fahey, P. F. (**1993**). "Asecond cochlear-frequency map that correlates distortion product and neural tuning measurements," J. Acoust. Soc. Am. **94**, 809–816.

Avan, P., Bonfils, P., Gilain, L., and Mom, T. (**2003**). "Physiopathological significance of distortion-product otoacoustic emissions at $2f1-f2$ produced by high- versus low-level stimuli," J. Acoust. Soc. Am. **113**, 430–441.

Bian, L. (**2004**). "Cochlear compression: Effects of low-frequency biasing on quadratic distortion product otoacoustic emission," J. Acoust. Soc. Am. **116**, 3559–3571.

Bian, L. (**2006**). "Spectral fine-structures of low-frequency modulated distortion product otoacoustic emissions," J. Acoust. Soc. Am. **119**, 3872–3885.

Bian, L., and Chertoff, M. E. (**2001**). "Distinguishing cochlear pathophysiology in 4-aminopyridine and furosemide treated ears using a nonlinear systems identification technique," J. Acoust. Soc. Am. **109**, 671–685.

Bian, L, and Scherrer, N. M. (**2007**). "Low-frequency modulation of distortion product otoacoustic emissions in humans," J. Acoust. Soc. Am. **122**, 1681–1692.

Bian, L., Chertoff, M. E., and Miller, E. (**2002**). "Deriving a cochlear transducer function from low-frequency modulation of distortion product otoacoustic emissions," J. Acoust. Soc. Am. **112**, 198–210.

Brown, A. M. (**1987**). "Acoustic distortion from rodent ears: A comparison of responses from rats, guinea pigs and gerbils," Hear. Res. **31**, 25–38.

Brown, A. M. (**1993**). "Distortion in the cochlea: Acoustic $f2-f1$ at low stimulus levels," Hear. Res. **70**, 160–166.

Brown, A. M., Gaskill, S. A., Carlyon, R. P., and Williams, D. M. (**1993**). "Acoustic distortion as a measure of frequency selectivity: Relation to psychophysical equivalent rectangular bandwidth," J. Acoust. Soc. Am. **93**, 3291–3297.

Carney, L. H. (**1993**). "A model for responses of low-frequency auditory-nerve fibers in cat," J. Acoust. Soc. Am. **93**, 401–417.

Dhar, S., Long, G. R., Talmadge, C. L., and Tubis, A. (**2005**). "The effect of stimulus-frequency ratio on distortion product otoacoustic emission components," J. Acoust. Soc. Am. **117**, 3766–3776.

Dreisbach, L. E., and Siegel, J. H. (**2005**). "Level dependence of distortion-product otoacoustic emissions measured at high frequencies in humans," J. Acoust. Soc. Am. **117**, 2980–2988.

Fahey, P. F., Stagner, B. B., and Martin, G. K. (**2006**). "Mechanism for bandpass frequency characteristic in distortion product otoacoustic emission generation," J. Acoust. Soc. Am. **119**, 991–996.

Fahey, P. F., Stagner, B. B., Lonsbury-Martin, B. L., and Martin, G. K. (**2000**). "Nonlinear interactions that could explain distortion product interference response areas," J. Acoust. Soc. Am. **108**, 1786–1802.

Frank, G., and Kössl, M. (**1996**). "The acoustic two-tone distortions $2f1-f2$ and $f2-f1$ and their possible relation to changes in the operating point of the cochlear amplifier," Hear. Res. **98**, 104–115.

Garner, C. A., Neely, S. T., and Gorga, M. P. (**2008**). "Sources of variability in distortion product otoacoustic emissions," J. Acoust. Soc. Am. **124**, 1054–1067.

Gaskill, S. A., and Brown, A. M. (**1990**). "The behavior of the acoustic distortion product, $2f1-f2$, from the human ear and its relation to auditory sensitivity," J. Acoust. Soc. Am. **88**, 821–839.

Gorga, M. P., Neely, S. T., Dorn, P. A., and Hoover, B. M. (**2003**). "Further efforts to predict pure-tone thresholds from distortion product otoacoustic emission input/output functions," J. Acoust. Soc. Am. **113**, 3275–3284.

Greenwood, D. D. (**1990**). "A cochlear frequency-position function for several species-29 years later," J. Acoust. Soc. Am. **87**, 2592–2605.

Harris, F. P., Lonsbury-Martin, B. L., Stagner, B. B., Coats, A. C., and Martin, G. K. (**1989**). "Acoustic distortion products in humans: Systematic changes in amplitude as a function of $f_2/f_1$ ratio," J. Acoust. Soc. Am. **85**, 220–229.

Hauser, R., and Probst, R. (**1991**). "The influence of systematic primary-tone level variation $L_2-L_1$ on the acoustic distortion product emissions $2f_1-f_2$ in normal human ears," J. Acoust. Soc. Am. **89**, 280–286.

Johnson, T. A., Neely, S. T., Garner, C. A., and Gorga, M. P. (**2006**) "Influence of primary-level and primary frequency ratios on human distortion product otoacoustic emissions," J. Acoust. Soc. Am. **119**, 418–428.

Kennedy, H. J., Crawford, A. C., and Fettiplace, R. (**2005**). "Force generation by mammalian hair bundles supports a role in cochlear amplification," Nature (London) **433**, 880–883.

Kim, D. O. (**1980**). "Cochlear mechanics: Implications of electrophysiological and acoustical observations," Hear. Res. **2**, 297–317.

Knight, R. D., and Kemp, D. T. (**2001**) "Wave and place fixed DPOAE maps of the human ear," J. Acoust. Soc. Am. **109**, 1513–1525.

Kummer, P., Janssen, T., Hulin, P., and Arnold, W. (**1998**). "The level and growth behavior of the $2\ f1-f2$ distortion product otoacoustic emission and its relationship to auditory sensitivity in normal hearing and cochlear hearing loss," J. Acoust. Soc. Am. **103**, 3431–3444.

Kummer, P., Janssen, T., Hulin, P., and Arnold, W. (**2000**). "Optimal $L_1-L_2$ primary tone level separation remains independent of test frequency in humans," Hear. Res. **146**, 47–56.

Lasky, R. E. (**1998**). "Distortion product otoacoustic emissions in human newborns and adults. I. Frequency effects," J. Acoust. Soc. Am. **103**, 981–991.

Liberman, M. C., Gao, J., He, D. Z. Z., Wu, X., Jia, S., and Zou, J. (**2002**). "Prestin is required for electromotility of the outer hair cell and for the cochlear amplifier," Nature (London) **419**, 300–304.

Londero, A., Bonfils, P., and Avan, P. (**2002**). "Magnitudes and phases of human distortion-product otoacoustic emissions at $2f_1-2f_2$ against $f_2/f_1$: Effects of an audiometric notch," Hear. Res. **167**, 46–56.

Lonsbury-Martin, B. L., and Martin, G. K. (**2003**). "Otoacoustic emissions," Curr. Opin. Otolaryngol. Head Neck Surg. **11**, 361–366.

Lukashkin, A. N., and Russell, I. J. (**1999**). "Analysis of the $f_2-f_1$ and $2f_1-2f_2$ distortion components generated by the hair cell mechanoelectrical transducer: Dependence on the amplitudes of the primaries and feedback gain," J. Acoust. Soc. Am. **106**, 2661–2668.

Lukashkin, A. N., and Russell, I. J. (**2001**). "Origin of the bell-like dependence of the DPOAE amplitude on primary frequency ratio," J. Acoust. Soc. Am. **110**, 3097–3106.

Martin, G. K., Stagner, B. B., and Lonsbury-Martin, B. L. (**2003**). "Difference-tone response areas in rabbits," in *Biophysics of the Cochlea: from Molecules to Models*, edited by A. W. Gummer, E. Dalhoff, M. Nowotny, and M. P. Scherer (World Scientific, Singapore), pp. 464–471.

Michaelis, C. E., Gehr, D. D., Deingruber, K., Arnold, W., and Lamm, K. (**2004**). "Optimum primary tone level setting for measuring high amplitude DPOAEs in guinea pigs," Hear. Res. **189**, 58–62.

Mills, D. M. (**1997**). "Interpretation of distortion product otoacoutic emission measurements. I. Two stimulus tones," J. Acoust. Soc. Am. **102**, 413–429.

Mills, D. M. (**2002**). "Interpretation of standard distortion product otoacoutic emission measurements in light of the complete parametric response," J. Acoust. Soc. Am. **112**, 1545–1560.

Mills, D. M., Feeney, M. P., Drake, E. J., Folsom, R. C., Sheppard, L., and Seixas, N. S. (**2007**). "Developing standards for distortion product otoacoutic emission measurements," J. Acoust. Soc. Am. **122**, 2203–2214.

Moulin, A. (**2000**). "Influence of primary frequency ratio on distortion product otoacoustic emissions amplitude. I. Intersubject variability and consequences on the DPOAE-gram," J. Acoust. Soc. Am. **107**, 1460–1470.

Neely, S. T., Johnson, T. A., and Gorga, M. P. (**2005**). "Distortion-product otoacoustic emission measured with continuously varying stimulus level," J. Acoust. Soc. Am. **117**, 1248–1259.

Nuttall, A. L., and Dolan, D. F. (**1993**). "Intermodulation distortion ($F_2-F_1$) in inner hair cell and basilar membrane responses," J. Acoust. Soc. Am. **93**, 2061–2068.

Patuzzi, R., and Moleirinho, A. (**1998**). "Automatic monitoring of mechano-electrical transduction in the guinea pig cochlea," Hear. Res. **125**, 1–16.

Pibal, I., Drexl, M., and Kössl, M. (**2002**). "Level dependence of optimal stimulus difference for evoking DPOAEs in the gerbil," Hear. Res. **174**, 260–263.

Rhode, W. S. (**2007**). "Distortion product otoacoustic emissions and basilar membrane vibration in the 6–9 kHz region of sensitive chinchilla cochleae," J. Acoust. Soc. Am. **122**, 2725–2737.

Robles, L., and Ruggero, M. A. (**2001**). "Mechanics of the mammalian cochlea," Physiol. Rev. **81**, 1305–1352.

Shera, C. A. (**2004**) "Mechanisms of mammalian otoacoustic emission and their implications for the clinical utility of otoacoustic emissions," Ear Hear. **25**, 86–97.

Stover, L. J., Neely, S. T., and Gorga, M. P. (**1999**). "Cochlear generation of intermodulation distortion revealed by DPOAE frequency functions in normal and impaired ears," J. Acoust. Soc. Am. **106**, 2669–2678.

Takahashi, S., and Santos-Sacchi, J. (**1999**). "Distortion component analysis of outer hair cell motility-related gating charge," J. Membr. Biol. **169**, 199–207.

Tubach, M., McGee, J. A., and Walsh, E. J. (**1996**). "Distortion generated by the ear: Its emergence and evolution during development," Laryngoscope **106**, 822–830.

Vento, B. A., Durrant, J. D., and Sabo, D. L. (**2004**). "Development of $f_2/f_1$ ratio functions in humans," J. Acoust. Soc. Am. **115**, 2138–2147.

Whitehead, M. L., Stagner, B. B., McCoy, M. J., Lonsbury-Martin, B. L., and Martin, G. K. (**1995**). "Dependence of distortion-product otoacoustic emissions on primary levels in normal and impaired ears. II. Asymmetry in $L_1$,$L_2$ space," J. Acoust. Soc. Am. **97**, 2359–2377.